Accepted Manuscript

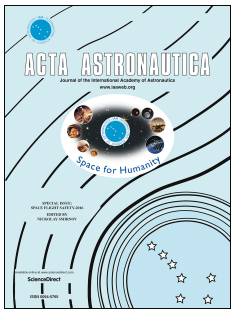

A concept of hazardous NEO detection and impact warning system

Toshinori Ikenaga, Yohei Sugimoto, Matteo Ceriotti, Makoto Yoshikawa, Toshifumi Yanagisawa, Hitoshi Ikeda, Nobuaki Ishii, Takashi Ito, Masayoshi Utashima

PII: S0094-5765(17)31524-2

DOI: 10.1016/j.actaastro.2018.06.058

Reference: AA 6977

To appear in: *Acta Astronautica*

Received Date: 30 October 2017

Revised Date: 27 April 2018

Accepted Date: 29 June 2018

Please cite this article as: T. Ikenaga, Y. Sugimoto, M. Ceriotti, M. Yoshikawa, T. Yanagisawa, H. Ikeda, N. Ishii, T. Ito, M. Utashima, A concept of hazardous NEO detection and impact warning system, *Acta Astronautica* (2018), doi: 10.1016/j.actaastro.2018.06.058.

5th IAA Planetary Defense Conference – PDC 2017
15-19 May 2017, Tokyo, Japan

IAA-PDC-17-00-P03
A CONCEPT OF HAZARDOUS NEO DETECTION AND IMPACT WARNING SYSTEM

Toshinori Ikenaga(1), Yohei Sugimoto(2), Matteo Ceriotti(3), Makoto Yoshikawa(4), Toshifumi Yanagisawa(5), Hitoshi Ikeda(6), Nobuaki Ishii(7), Takashi Ito(8) and Masayoshi Utashima(9)

(1)JAXA/RDD, *2-1-1, Sengen, Tsukuba, Ibaraki, 305-8505, Japan, +81 (0) 50 3362 4109, Ikenaga.toshinori@jaxa.jp*
(2)JAXA/RDD, *2-1-1, Sengen, Tsukuba, Ibaraki, 305-8505, Japan, +81 (0) 50 3362 8898,* sugimoto.yohei@jaxa.jp
(3)University of Glasgow, *University Avenue, Glasgow, G12 8QQ, United Kingdom, +44 (0) 141 330 6465, Matteo.Ceriotti@glasgow.ac.uk*
(4)JAXA/ISAS, *3-1-1, Yoshinodai, Chuoku, Sagamihara, Kanagawa, 252-5210, Japan, +81 (0) 50 3362 3983,* yoshikawa.makoto@jaxa.jp
(5)JAXA/RDD, *7-44-1, Jindaijihigashimachi, Chofu, Tokyo, 182-0012, Japan, +81 (0) 50 3362 5927, yanagisawa.toshifumi@jaxa.jp*
(6)JAXA/RDD, *2-1-1, Sengen, Tsukuba, Ibaraki, 305-8505, Japan, +81 (0) 50 3362 4143, ikeda.hitoshi@jaxa.jp*
(7)JAXA/ISAS, *3-1-1, Yoshinodai, Chuoku, Sagamihara, Kanagawa, 252-5210, Japan, +81 (0) 50 3362 3591,* ishii.nobuaki@jaxa.jp
(8)NAOJ/CfCA, *2-21-1, Osawa, Mitaka, Tokyo, 181-8588, Japan, +81 (0) 422 34 3845, tito@cfca.nao.ac.jp*
(9)JAXA/RDD, *2-1-1, Sengen, Tsukuba, Ibaraki, 305-8505, Japan, +81 (0) 50 3362 6262, utashima.masayoshi@jaxa.jp*

Keywords: *NEO, Space telescope, Planetary defense, Sun-Earth L1, Artificial Equilibrium Point.*

Nomenclature

a	:	semi-major axis in au
a_E	:	semi-major axis of Earth orbit in au
$\vec{a}_{aep}$	:	acceleration to keep AEP
α	:	phase angle AEP w.r.t Sun-Earth line
b	:	Azimuth angle
D	:	Size of NEO
D_{ap}	:	Aperture diameter
e	:	eccentricity
ε	:	ratio of light intensity
El	:	Elevation angle
Φ	:	potential by centrifugal force
G	:	slope parameter
H	:	absolute magnitude
i	:	inclination
J_1	:	limit magnitude at 1 second integration
l	:	Elevation angle

m_1	:	mass of primary body
m_2	:	mass of secondary body
P	:	orbital period
q	:	perihelion distance
Q	:	apherihelion distance
$\vec{r}$	:	position vector of SC w.r.t. CG
$\vec{r}_1$	:	position vector of Primary w.r.t. CG
$\vec{r}_2$	:	position vector of Secondary w.r.t. CG
$\vec{r}_L$	:	position vector of Lagrange point w.r.t. CG
$T_{warning}$	:	warning time
V_∞	:	V-infinity
μ^*	:	ratio of gravitational constants
μ_S	:	Earth's gravitational constant
μ_1	:	Primary's gravitational constant
μ_2	:	Secondary's gravitational constant
U	:	potential
U^*	:	pseudo potential
V_E	:	Earth's velocity
$\vec{\omega}$	:	angular velocity vector around CG
X	:	X axis of coordinate system
Y	:	Y axis of coordinate system
Z	:	Z axis of coordinate system

Acronyms/Abbreviations

au	astronomical unit e.g. 149,597,870,700 m
AEP	Artificial Equilibrium Point
APAON	Asia-Pacific Asteroid Observation Network
ATLAS	Asteroid Terrestrial-impact Last Alert System
BSGC	Bisei Spaceguard Center
CG	Center of Gravity
CR3BP	Circular Restricted Three-body Problem
COPUOS	Committee on the Peaceful Uses of Outer Space
CSA	Canada Space Agency
CSS	Catalina Sky Survey
DLR	Deutsches Zentrum für Luft- und Raumfahrt
DND	Department of National Defense
DRDC	Defence Research and Development Canada
DRO	Distant Retrograde Orbit
ESA	European Space Agency
ESTEC	European Space Research and Technology Centre
FOV	Field-of-View
HEOSS	High Earth Orbit Space Surveillance
HST	Hubble Space Telescope
IAWN	International Asteroid Warning Network
IEO	Inner Earth Object
IGD	Institute of Geosphere Dynamics
IR	Infrared
IRAS	Infra-Red Astronomy Satellite
IRC	Infrared Camera

ISAS	Institute of Space and Astronautical Science
JAXA	Japan Aerospace Exploration Agency
JPL	Jet Propulsion Laboratory
JSGA	Japan Spaceguard Association
JWST	James Webb Space Telescope
LINEAR	Lincoln Laboratory's Near-Earth Asteroid Research
LONEOS	Lowell Near-Earth Object Survey
MOID	Minimum Orbit Intersection Distance
NASA	National Aeronautics and Space Administration
NEAT	Near-Earth Asteroid Tracking
NEA	Near Earth Asteroid
NEC	Near Earth Comet
NEO	Near Earth Object
NEOCam	Near Earth Object Camera
NEOPOP	Near Earth Object Population Observation Program
NEOSSat	Near Earth Object Surveillance Satellite
NESS	Near Earth Space Surveillance
NOAA	National Oceanic and Atmospheric Administration
OD	Orbit Determination
PAIR	Probabilistic Asteroid Impact Risk
PDCO	Planetary Defense Coordination Office
PHO	Potentially Hazardous Object
POD	Precise Orbit Determination
SC	Spacecraft
SEL1	Sun-Earth Lagrange point 1
SEL2	Sun-Earth Lagrange point 2
SMPAG	Space Mission Planning Advisory Group
SODA	System of Observation of Day-Time Asteroids
SSO	Sun Synchronous Orbit
TOF	Time-of-Flight
UN	United Nation
VI	Virtual Impactor
WISE	Wide-field Infrared Survey Explorer

Abstract

In 2013, the well-known Chelyabinsk meteor entered the Earth's atmosphere over Chelyabinsk, Russia. It is estimated that the meteor exploded at altitude near 30 km[2], which damaged thousands of buildings and injured a thousand of residents[3-4]. The estimated size of the meteor is approximately 20 m[2]. Because the meteor approached to Earth from Sun direction, no ground-based observatories could not detect until the impact.

Considering such situations, the paper proposes a concept to detect Chelyabinsk-class small Near-Earth Objects. The concept addresses a "last-minute" warning system of NEO impact, in the same manner of "Tsunami" warning.

To achieve the mission objective, two locations are assumed for the space telescope installation point i.e., Sun-Earth Lagrange point 1, SEL1 and Artificial Equilibrium Point, AEP. SEL1 is one of the natural equilibrium points, on the other hand, AEP is artificially equilibrated point by Sun and Earth gravity, centrifugal force and low-thrust

acceleration. The magnitude of the acceleration to keep AEP is sufficiently small near 1 au radius orbit around the Sun i.e., the order of μm/s^2 which can be achieved by solar sail. Through some cases of numerical simulations considering the size of NEOs and detector capability, this paper will show the feasibility of the proposed concept.

Introduction

The hazard mitigation caused by NEOs is a growing interest. The well-known Tunguska event occurred in Russia in 1908[1], and the Chelyabinsk meteor event in 2013 reminded mankind that the threats of NEO impacts still exists on Earth. In the Chelyabinsk event, an NEO with the size of approximately 20 m in diameter entered Earth's atmosphere over Chelyabinsk, Russia., It is estimated that the meteor exploded at altitude near 30 km[2]. The event damaged more than 7,300 buildings and injured about 1,500 residents[3]. The air-burst of the meteor is estimated to have an energy equivalent of approximately 500 kt of TNT[2], which is about 30 times larger than that of the atomic bomb detonated over Hiroshima. As of today, it is recognized as one of the most significant terrestrial impact events in modern times.

The threats of NEO impacts has also been discussed in the United Nations (UN). The first international conference on the NEO hazard mitigation was convened in the UN in 1995, and the UN has established two organizations: International Asteroid Warning Network, IAWN and Space Mission Planning Advisory Group, SMPAG in 2013[8-10]. In addition to such international framework conducted in the UN, NASA announced to launch the Planetary Defense Coordination Office, PDCO. PDCO is responsible for the followings[11]:

- Ensuring the early detection of potentially hazardous objects (PHOs) – asteroids and comets whose orbit are predicted to bring them within 0.05 Astronomical Units of Earth; and of a size large enough to reach Earth's surface – that is, greater than perhaps 30 to 50 meters;

- Tracking and characterizing PHOs and issuing warnings about potential impacts;

- Providing timely and accurate communications about PHOs;

- Performing as a lead coordination node in U.S. Government planning for response to an actual impact threat.

According to the definition of Jet Propulsion Laboratory, JPL, NEO is defined as the asteroids and comets whose perihelion distance, q is less than 1.3 au. NEO consists of Near Earth Asteroid, NEA and Near Earth Comment, NEC. NEC is defined as the comets whose orbital period, P is less than 200 years. NEA is NEO other than NEC. NEA consists of four groups i.e., Atira, Aten, Apollo and Amor, according to the q, aphelion distance, Q and their semi-major axes, a. PHOs are the asteroids and comet nuclei whose Minimum Orbit Intersection Distance, MOID is within 0.05 au. The absolute magnitude, H of PHO is defined within 22 which is larger than 140 m in size[5]. However, it should be noted that the smaller size objects are of significant interest because they are more order of numerous than larger size objects, are more difficult to detect, and will likely provide much shorter warning times between discovery and impact[5].

Figure 1 shows the estimated population of NEAs[6]. Specifically, the completion versus size of present surveys based on the re-detection ratio is estimated, using a large set of synthetic orbital elements matching as best possible the distribution of the real NEA population[7]. For example, when the populations of H = 22 (ca. 140 m size) and H = 26 (ca. 20 m size) are compared, the estimated number of H = 22 is roughly 10^4, while that of H = 24 is roughly 10^6, which is twice larger in magnitude. Besides, the impact interval of H = 24 is about 100 years which is much more frequent than that of H = 22.

Many ground-based NEO survey programs are being conducted such as Spacewatch, Near-Earth Asteroid Tracking(NEAT), Lowell Near-Earth Object Survey(LONEOS), Lincoln Laboratory's Near-Earth Asteroid Research(LINEAR), Catalina Sky Survey(CSS)[12]. Asteroid Terrestrial-impact Last Alert System, ATLAS is also the ground-based observatories consisting of two observatories located in Hawaii. As the name indicates, ATLAS focuses on to detect "small (10–140m) asteroids on their 'final plunge' toward impact with Earth"[21]. ATLAS has been fully operated since 2017, and can cover 13,000 deg^2 at least four times per night[16]. In Japan, Bisei Spaceguard Center, BSGC was constructed in 1999 to track asteroids and space debris, and is operated by Japan Spaceguard Association, JSGA, which funded by Japan Aerospace Exploration Agency, JAXA[14]. In 2013, Yoshikawa proposed to establish Asia-Pacific Asteroid Observation Network, APAON, which started in 2014[15].

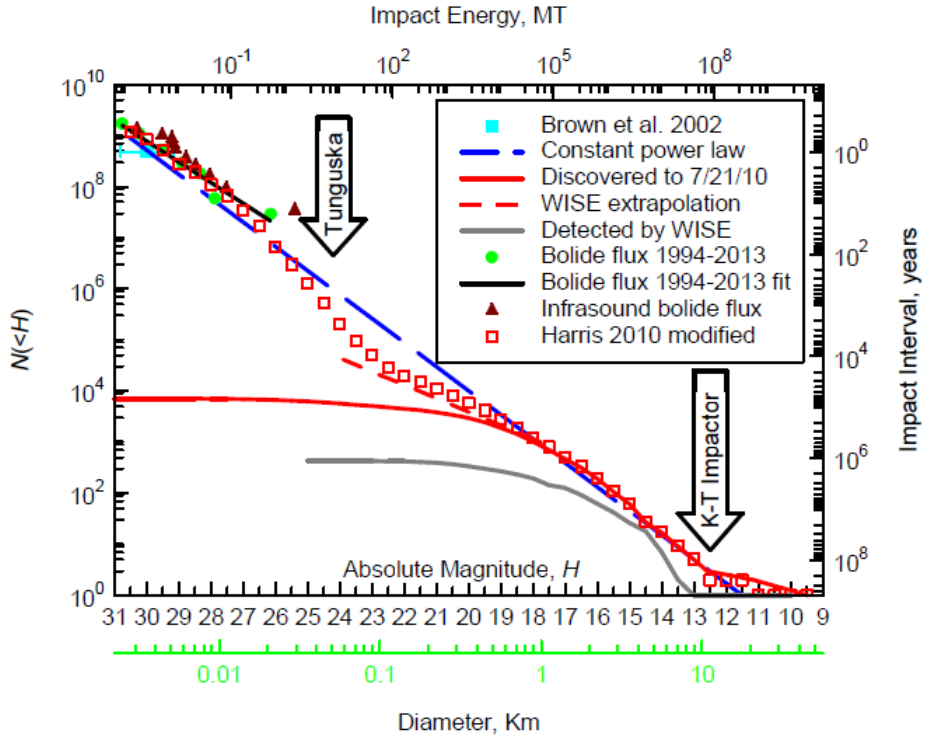

Fig. 1 NEO population and impact interval[6]

Space-based NEO survey missions are also being carried out or planed. In December of 2009, Wide-field Infrared Survey Explorer, WISE was launched into an about 500 km altitude down-dusk Sun Synchronous Orbit, SSO[17, 18]. After the completion of the primary mission, NEO survey, called NEOWISE, started as the

extended mission of WISE. The first NEOWISE survey (before the hibernation of the spacecraft) had been conducted until February 1st 2011. During the first NEOWISE survey, more than 130 new NEOs were discovered[18]. Canadian Near Earth Object Surveillance Satellite, NEOSSat is the joint microsatellite project between the Canadian Space Agency, CSA and Defence Research and Development Canada, DRDC, and was launched in February 2013[20]. NEOSSat is 75 kg microsatellite equipped with 15 cm Cassegrain telescope which is able to detect 20 magnitude objects with a 100 sec exposure[19]. NEOSSat incorporates two missions: DND's space surveillance mission (High Earth Orbit Space Surveillance – HEOSS) and CSA's asteroid finding mission (Near Earth Space Surveillance – NESS). NESS by NEOSSat focuses on to detect so-called Inner Earth Objects, IEOs such as Aten-class or Atila-class[20]. Planetary resources Inc. proposes CubeSat-class space telescope for NEO survey[21]. On January 12, 2018, Arlkyd 6 was launched, which is the first successful launch of Planetary resources Inc[22]. The Japanese infrared all-sky survey satellite, AKARI was developed and launched in 2006 by the Institute of Space and Astronautical Science, ISAS of JAXA. The primary purpose of AKARI is to provide second-generation infrared catalogues so as to obtain a better spatial resolution and a wider spectral coverage than the first catalogues produced by the Infra-Red Astronomy Satellite, IRAS[23]. AKARI is not dedicated to NEO survey; however the all-sky survey by the Infrared Camera, IRC of AKARI provided more than twenty thousand thermal infrared observations of over five thousand asteroids[24].

Table 1 Space-based telescopes for NEO survey

Mission	Launch	Location	Aperture	mass	Organization
NEOWISE	2009	SSO	0.4 m (IR)	661 kg	NASA/JPL
NEOSSat	2013	SSO	0.15 m	74 kg	CSA, DRDC
Arlkyd 6	2018	SSO	below 0.1 m	10 kg	Planetary resources Inc.
AKARI*	2006	SSO	0.7 m (IR)	952 kg	JAXA/ISAS
NEOCam	proposed: 2021	SEL1 or orbit near Venus	0.5 m (IR)	unknown	NASA/JPL
Sentinel	canceled	orbit near Venus	0.5 m (IR)	1500 kg	B612 foundation
Earthguard-I	not proposed	orbit near Mercury	0.2-0.25 m	140 kg(solar sail option)	Kayser-Threde GmbH, DLR
JWST*	planed: 2020	SEL2	6.6 m (IR)	6500 kg	NASA, ESA, CSA

* Note: AKARI and JWST are not dedicated to NEO survey mission.

For the future space-based missions, Near Earth Object Camera, NEOCam is proposed by NASA. NEOCam is an infrared space telescope using Sun-Earth Lagrange point 1[25]. B612 foundation proposed Sentinel space telescope which is an infrared telescope with 50 cm aperture. It was intended to survey NEOs from Venus-like orbit[26]. However, it was cancelled and replaced by NEOCam. German Aerospace Center, DLR also carried out a Phase A study of Earthguard-I under contract to European Space Agency, ESA[27, 28]. Earthguard-I is assumed to detect IEOs from a heliocentric orbit of a = 0.5 au. A piggy-back option of BepiColombo, which is the joint Mercury exploration mission between ESA and JAXA, was considered in the study. Solar sail was also investigated as an alternative option for trajectory transfer[28]. NASA's James Webb Space Telescope, JWST will also contribute to NEO survey. JWST is the scientific successor to the Hubble Space Telescope, HST[30]. JWST is equipped with approximately 6.6 m aperture infrared telescope and will be located on Sun-Earth Lagrange point 2, SEL2[29, 30]. JWST is

anticipated to provide the opportunity for ground-breaking observations of asteroids[31]. Table 1 summarizes the space-based telescope missions for NEO survey. As shown in Table 1, the orbits of all four satellites under operation are SSO, while the future missions are intended to use SEL1, SEL2, Venus-like orbit or heliocentric orbit near Mercury.

Figure 2 shows the history of the number of NEOs discovered by survey missions as of 2017[13]. CSS and Pan-STARRS occupy most of the recent discoveries.

Other than the future mission plans or proposals shown in Table 1, there some concept studies for NEO detection missions. Stramacchia et al analyzed a concept for the NEO detection from Distant Retrograde Orbit, DRO belonging to Family-f stable orbits around the secondary body in Circular Restricted Three-Body Problem, CR3BP of Sun-Earth system[32]. Stramacchia et al evaluated the mission performance based on H and G Magnitude System from the perspectives of the coverage area and warning time, which is the time between the detection and Earth impact. Perrozi et al proposed a concept using DRO of Earth-Moon system[33].

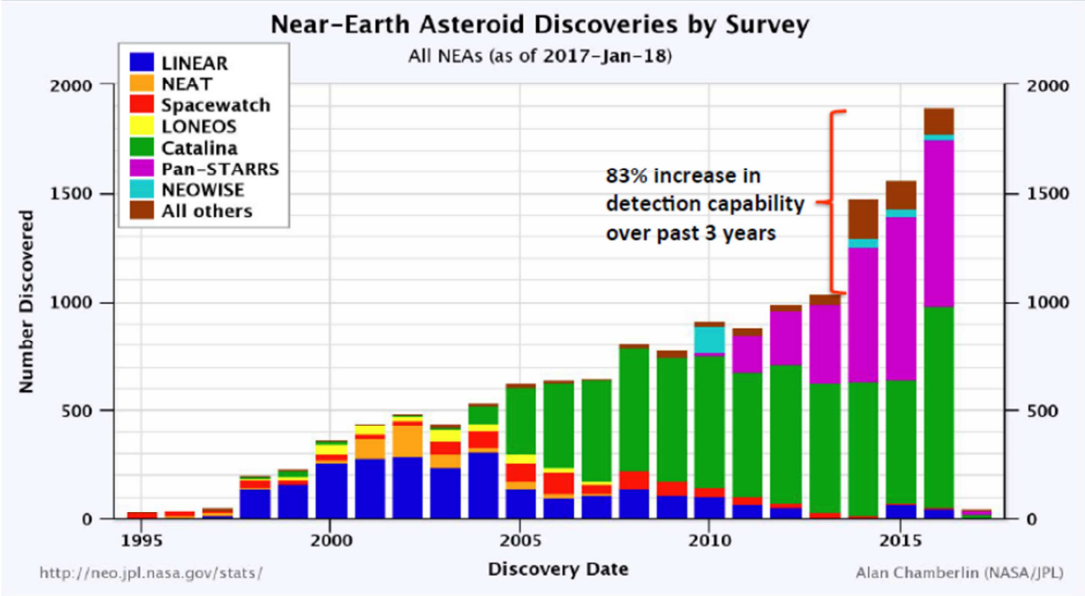

Fig. 2 Near-Earth Asteroid Discoveries[13]

In Russia, which experienced two major meteor impact events in modern times, the Institute of Astronomy of the Russian Academy of Sciences is studying the System of Observation of Day-time Asteroids, SODA. SODA is dedicated to detect NEOs approaching from the Sun direction just like Chelyabinsk meteor. SODA is located around SEL1 and surveils Earth direction[34, 35].

The authors also studied on similar concept as the Russian SODA concept[36]. The concept in the paper is dedicated to detect NEOs approaching from the Sun direction, and once an impacting NEO is detected, the system raises an alert for evacuation. For this purpose, a space telescope is located at SEL1 and surveils the Sun direction as described in Figure 3. The mission performance was evaluated based on H and G Magnitude System using about 25,000 Virtual Impactors, VIs[36].

In the SEL1 mission concept, it is assumed that the ground-based observatories surveys the night-side, therefore the space-based telescope located at SEL1 surveys the noon-side as shown in Figure 3. However, telescopes should avoid to see the Sunlight directly, hence it is assumed that the space telescope has a hood which is 4 times longer than the aperture diameter i.e., the space telescope is assumed to be able to observe the noon-side except about 15 deg from the Sun direction which is called “Sun avoidance angle” in the paper. The results of the mission performance evaluation conducted in the paper showed that even a telescope of J_1 = 24 can detect roughly 40% of 50 m VIs and 50% of 140 m VIs at 0.1 au distance to Earth (See Table 6), where J_1 is the limiting magnitude at 1 sec integration used to define the detector’s performance in this study. In the simulation, VIs are produces based on Bottke model. Bottke model is the debiased NEO population model which was calibrated by fitting to 138 NEOs discovered or accidentally re-discovered by Spacewatch at that time[37]. Granvik et al published new NEO population model in 2016[38]. Granvik model is based on more than 4,000 NEOs discovered or re-discovered by CSS, and is calibrated from H = 15 up to H = 25[38, 39].

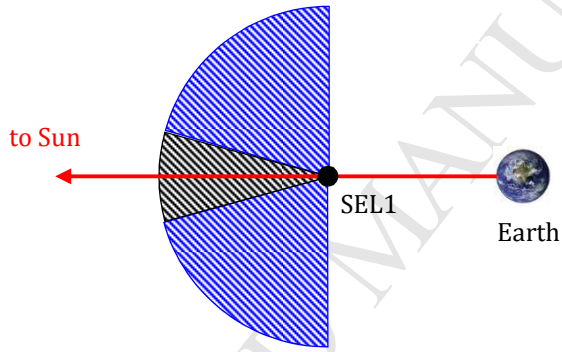

Fig. 3 Overview of SEL1 option[36]

25,000 VIs were produced based on Bottke model for the SEL1 mission concept study of [36]. Based on the VIs, the Time-of-Flight, TOF is calculated for NEO to impact Earth from a distance. Table 2 summarizes TOF in the cases of 0.1-0.5 au distances from NEO to Earth. Note that minimum TOF of Table 2 corresponds to a few NEOs orbiting retrograde around the Sun.

Table 2 TOF to Earth Impact

Distance from NEO to Earth	Average TOF	Minimum TOF
0.5 au	22.7 days	18.1 days
0.4 au	20.2 days	14.7 days
0.3 au	16.9 days	11.1 days
0.2 au	12.7 days	7.5 days
0.1 au	6.9 days	3.8 days

As shown in Table 2, the above 0.1 au corresponds to about 7 days in average before Earth impact. In other word, if NEO is detected by 0.1 au distance to Earth, we will be able to have roughly 7 days to prepare the impact including Orbit Determination, OD process. In this paper, the time from NEO detection to Earth impact is defined as warning time, $T_{warning}$. This paper assumes “warning” process as follows;

- Detection, initial OD and evaluation of impact possibility.

- Decision make if necessary.

- Public release, start evacuation.

Although it should be discussed how long $T_{warning}$ is necessary to complete the evacuation, it is hard to tell the appropriate number of $T_{warning}$. Many factors should be considered such as the impact location, the phenomena at the impact, and so on. Many studies are carried out to assess the meteor risk. For example, Mathias et al presented Probabilistic Asteroid Impact Risk, PAIR assessment model[40]. The PAIR model can estimate the ground damage and affected population by meteor impact. The necessary $T_{warning}$ will vary widely by the result of the risk assessment.

Another important factor to determine $T_{warning}$ is OD. OD is essential process to evaluate the impact possibility, and if it impacts, we have to know where the meteor impacts with sufficient precision to raise alert properly. The analysis of OD is not the scope of this paper, however it is assumed as following OD process;

- Space telescope detect approaching objects by 0.1 au at nearest (roughly 7 days before impact)

- Initial OD is carried out using angle-only data provided by the space telescope, and the impact possibility is assessed.

- If it is potential impact, the radar observatories such as Arecibo and Goldstone start the precise OD.

According to [11], Arecibo and Goldstone can detect 20 m size of objects with 10-30 SNR for radar echoes at roughly 0.05 au. However, note that the detail condition such as the slope parameter of the object, or the rotation speed are not provided. From the above reasons, we set 0.1 au distance to Earth, which roughly corresponds to $T_{warning}$ = 7 days, as the threshold of NEO detection. The study on the space-telescope system design is out of scope of this paper; however it is assumed the tracking data is compressed on-board and downlink to the ground stations, and the orbit determination is conducted on the ground.

The SEL1 option in the previous study showed the limitation to detect NEOs[36]. As also mentioned in the other study[32], there is the exclusion zone where telescopes cannot detect NEOs due to the worse phase angle which makes NEOs fainter. To solve this problem, this paper proposes to use Artificial Equilibrium Point, AEP for the location of space telescopes. In the natural equilibrium points such as Lagrange points, three kinds of forces are balanced i.e., the gravitational forces by the primary and secondary bodies and centrifugal force. AEP, on the other hand, is an “artificial” equilibrium point where the residual acceleration is cancelled by low-thrust. Especially on a 1 au circular orbit around the Sun, the AEP can be maintained by very small acceleration, which enables to place the space telescope at an arbitrary fixed point relative to the Earth. Figure 4 shows the overview of AEP option. It is assumed to survey 30 deg half angle region once per day.

As for the detector, it is assumed to use the new method for the detection of fast-moving objects developed by JAXA[41]. The method was originally developed to detect debris around Earth, however it is also effective to detect fast-moving NEOs. In fact, JAXA discovered two new asteroids “2018EZ2” and “2018FH1” by JAXA’s 25 cm visible telescope located at Siding Spring, Australia, in March 2018[42]. Hence it is assumed to use visible telescope in this study. The mission performance of the AEP option is evaluated using VIs based on Bottke model considering different detector performance.

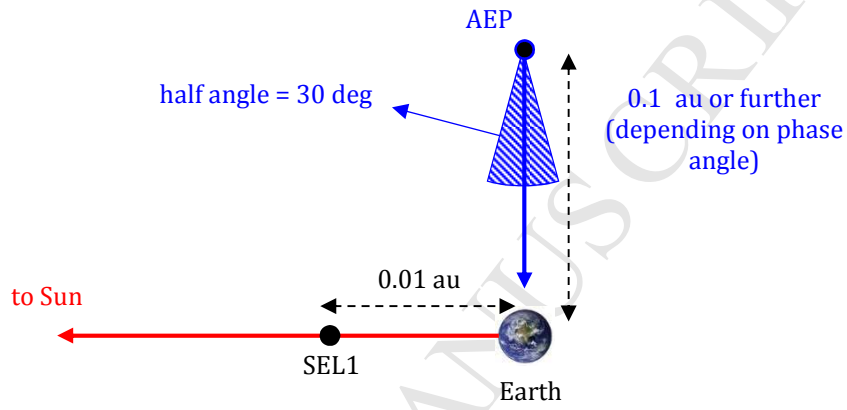

Fig. 4 Overview of AEP option

Virtual Earth Impactors

This study uses same VIs used in[36]. VIs for this study are produced based on Bottke model. All VIs impact to Earth at the epoch when Earth is at $(x, y, z) = (1\ \mathrm{au}, 0, 0)$ in the heliocentric inertial ecliptic frame. Note that the Earth’s orbit is assumed to be the circular orbit around the Sun with the radius of 1 au in this study. Once Keplerian elements of VIs are determined based on Bottle model, V-infinity vector at Earth impact is described as following;

$$\vec{V}_\infty = \sqrt{\frac{\mu_S}{a_E}} \begin{bmatrix} \pm\sqrt{2 - \frac{a_E}{a} - \frac{a(1-e^2)}{a_E}} \\ \sqrt{\frac{a(1-e^2)}{a_E}}\cos i - 1 \\ \pm\sqrt{\frac{a(1-e^2)}{a_E}}\sin i \end{bmatrix} \quad (1)$$

where a_E is the semi-major axis of Earth’s orbit, and a, e and i are the semi-major axis, eccentricity and inclination of the NEO of interest. Note that the V-infinity vector described by Equation (1) is in the Sun-Earth fixed coordinate of the epoch of interest, which is not a rotational frame. As Equation (1) indicates, there are four kinds of V-infinity vectors with respect to a combination of a, e and i. The signs of X and Z components of Equation (1) correspond to two kinds of eccentricity vectors, and the ascending or descending intersection points, respectively.

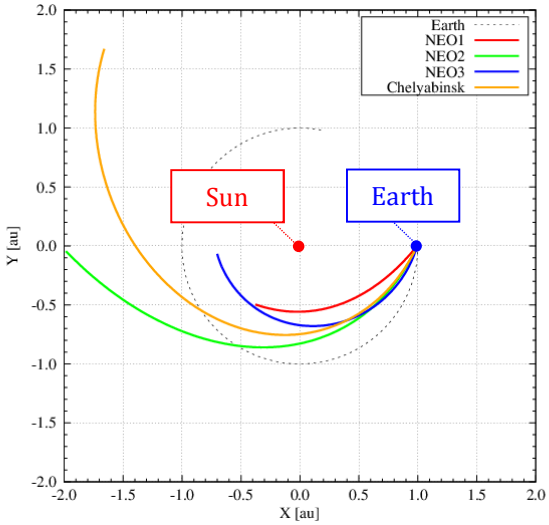

Fig. 5 Example orbits of VIs in Heliocentric inertial frame

2-body problem is assumed to describe VI's orbital motion i.e., only Sun's gravity is assumed. To produce VI's orbit, the V-infinity vector is added to the Earth's velocity vector at the impact epoch i.e., $(\dot{x}, \dot{y}, \dot{z}) = (0, V_{E,} 0)$ where V_E is the Earth's velocity which is about 30 km/s. Once the VI's state vector at Earth impact is obtained, the orbit is produced backwardly until the distance between VI and Earth reaches 1 au, or, the backward TOF reaches 1,000 days. Figures 5 and 6 show example orbits of VIs as viewed in the heliocentric inertial frame and the geocentric Sun-Earth fixed frame, respectively. Table 3 summarizes the parameters of the example VIs. Almost all of VIs stop at 1 au from Earth. "NEOs 1~3" appearing in Figures 5 and 6, and Table 3 correspond to "averaged V-infinity + 1σ," "averaged V-infinity," and "averaged V-infinity - 1σ," respectively. The parameters of Chelyabinsk is based on the information of the paper[3]. According to the paper, Institute of Geosphere Dynamics, IGD and Institute of Astronomy determined the orbit of Chelyabinsk meteor using the video records linking to the meteor[3].

Table 3. Parameters of example orbits.

Name	a [au]	e	i [deg]	V_∞ [km/s]
NEO1	3.39	0.83	7.50	24.61
NEO2	2.70	0.71	2.50	16.56
NEO3	0.92	0.28	2.50	8.19
Chelyabinsk[3]	1.77	0.58	4.30	15.56

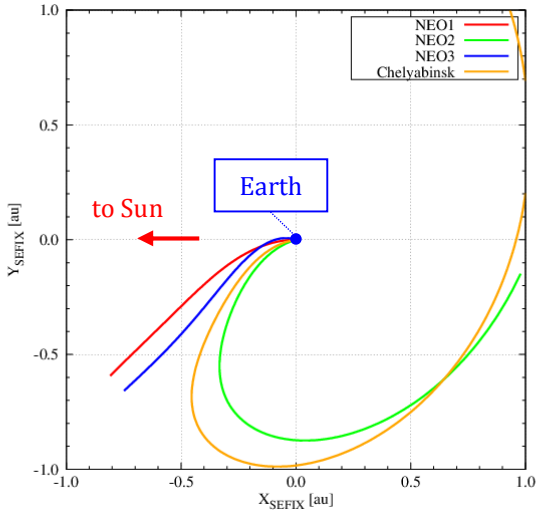

Fig. 6 Example orbits of VIs in Geocentric Sun-Earth fixed frame

The total number of VIs in this simulation is 24,527 for this study. Figure 7 shows the distribution of the VIs in an a-e map. As shown in Figure 6, the population of the VIs concentrates around a point where a = 2 au and e = 0.5 in the a-e map.

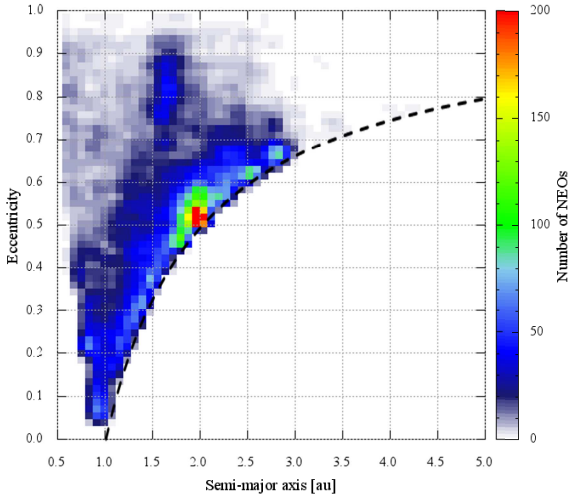

Fig. 7 Distribution of virtual Earth impactors based on Bottke model in an a-e map.

AEP Orbit

In CR3BP, the Sun and the Earth are assumed to have circular orbit around their common center of mass and to gravitationally attract the spacecraft whose mass is negligible i.e., will not affect the orbits of the two massive bodies. Figure 8 shows the geometry.

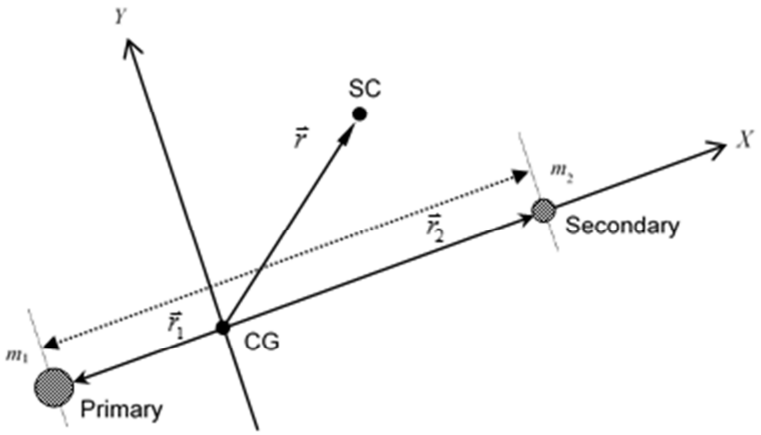

Fig. 8. Rotating Frame and Geometry of CR3BP

The equation of motion in CR3BP is described as following:

$$\frac{d^2\vec{r}}{dt^2} + 2\vec{\omega} \times \frac{d\vec{r}}{dt} + \vec{\omega} \times (\vec{\omega} \times \vec{r}) = -\nabla U(\vec{r}) \tag{2}$$

where $\vec{\omega}$ is the angular velocity vector around CG, and U is the gravitational potential by two celestial bodies as following:

$$U(\vec{r}) = -\left(\frac{1-\mu^*}{r_1} + \frac{\mu^*}{r_2}\right) \tag{3}$$

where μ^* is the ratio of the gravitational constants described as following:

$$\mu^* = \frac{m_2}{m_1 + m_2} \tag{4}$$

where m_1 and m_2 are the masses of Primary and Secondary. The gravitational constants of the two bodies, μ_1 and μ_2 are;

$$\mu_1 = 1 - \mu^*, \mu_2 = \mu^* \tag{5}$$

The third term of the left-hand side of Equation (2) is the potential by the centrifugal force which is describe as following:

$$\Phi(\vec{r}) = -\frac{1}{2}|\vec{\omega} \times \vec{r}|^2 \tag{6}$$

When the pseudo potential is defined as following:

$$U^*(\vec{r}) = U(\vec{r}) + \Phi(\vec{r}) \tag{7}$$

Then the natural equilibrium points i.e., Lagrange points are obtained from the following:

$$\nabla U^*(\vec{r}_L) = 0 \tag{8}$$

where $\vec{r}_L$ is the position vector of a Lagrange point. On the other hand, AEP is the point equilibrated by an artificial acceleration, $\vec{a}_{aep}$, which satisfies the following:

$$\nabla U^*(\vec{r}_{AEP}) - \vec{a}_{AEP} = 0 \tag{9}$$

Then, the required acceleration for the AEP is described as follows [43]:

$$\begin{cases} a_x = -x_0 + \dfrac{\mu_1}{{r_1}^3}(x_0 + \mu_2) + \dfrac{\mu_2}{{r_2}^3}(x_0 - \mu_1) \\ a_y = -y_0 + \dfrac{\mu_1}{{r_1}^3} y_0 + \dfrac{\mu_2}{{r_2}^3} y_0 \\ a_z = \dfrac{\mu_1}{{r_1}^3} z_0 + \dfrac{\mu_2}{{r_2}^3} z_0 \end{cases} \tag{10}$$

The in-plane acceleration with respect to the polar coordinate is described as the following:

$$\begin{cases} a_x(\alpha, r) = \mu^* - r\cos\alpha + \dfrac{1-\mu^*}{r^2}\cos\alpha + \mu^*(r\cos\alpha - 1)(1 - 2r\cos\alpha + r^2)^{-\frac{3}{2}} \\ a_y(\alpha, r) = -r\sin\alpha + \dfrac{1-\mu^*}{r^2}\sin\alpha + \mu^* r\sin\alpha\,(1 - 2r\cos\alpha + r^2)^{-\frac{3}{2}} \end{cases} \tag{11}$$

where α is the angle defined in Figure 9.

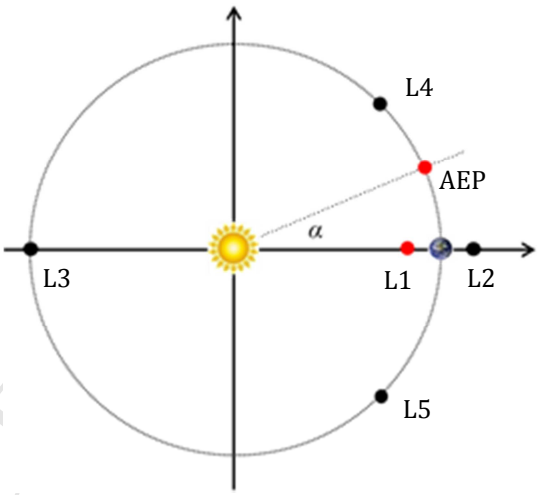

Fig. 9 Definition of α

Figure 10 shows the acceleration to keep AEP in the function of α. Note that r = 1 au. For reference, the order of acceleration of Japanese Hayabusa explorer is about 30 μm/s^2, and the one of Icarus solar sailor is 3.3 μm/s^2.

H and G Magnitude System

As mentioned in Introduction, it is assumed to use visible telescope in this study. The same method as [36] i.e., H and G Magnitude System is used to compute the size and visual magnitude of NEO[44]. The absolute magnitude is a scale of luminosity of a celestial body. Smaller size object has larger absolute magnitude, which means fainter in brightness. The absolute magnitude, H is described as following;

$$H = 17.75 - 5\log_{10} D \tag{12}$$

where D is the diameter of NEO in km. Note that the absolute magnitude of D = 1 km NEO corresponds to 17.75 since the mean NEO albedo is 0.14[44]. On the other hand, the visual magnitude, V is determined by the geometric relationship between the Sun, NEO and space-telescope, which is described as the following;

$$V = H + 5\log_{10}(d \cdot r) - 2.5\log_{10}\left((1-G)\Phi_1 + G\Phi_2\right) \tag{13}$$

where d is the distance in au between NEO and the telescope, r is the heliocentric distance in au of NEO. G is the slope parameter. Φ_i is the function of the phase angle β, which is described as the following;

$$\Phi_i = \exp\left(-A_i\left(\tan\frac{\beta}{2}\right)^{\beta_i}\right) \tag{14}$$

where A_1 = 3.33, A_2 = 1.87, B_1 = 0.63 and B_2 = 1.22. Figure 11 shows the definition β.

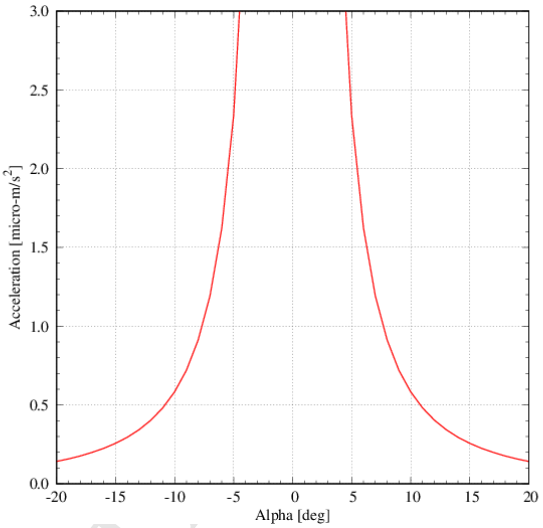

Fig. 10 AEP acceleration in the function of α

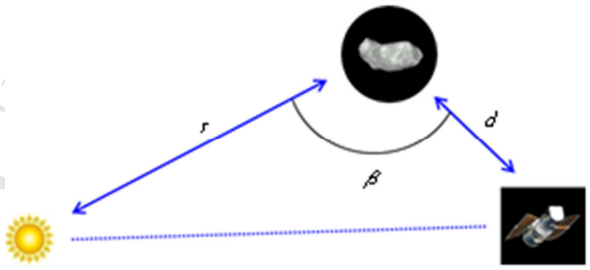

Fig. 11 Definition of β

When the limit magnitude at 1 sec integration, J_1 is introduced to describe the detector's performance, the limiting magnitude at Δt integration is described as following;

$$J = J_1 + \frac{\log_{10}\left(\frac{\Delta t}{1\ \mathrm{sec}}\right)}{0.8} \tag{15}$$

However, the noise by the zodiacal light should be considered from the perspective of practical mission design. It is assumed that the detectable magnitude improves with the square root of the integration time. In this assumption, the detectable magnitude is described as the following;

$$J = J_1 + \Delta J = J_1 + \frac{\log_{10}\left(\frac{\Delta t}{1\ \mathrm{sec}}\right)}{0.4} \tag{16}$$

Simulation Configuration of AEP Option

As described in Figure 4, it is assumed to locate a space telescope at AEP in this study. And the mission performance of AEP option is evaluated and compared with SEL1 option of the paper[36]. Three different size of VIs are assumed i.e., 25 m/50 m/140 m as summarized in Table 4[11]. The size of all VIs are set to the same value. For example, in the case of D = 25 m, all of about 25,000 VIs is set to 25 m. Hence three simulations are run in this study to evaluate the performance to the three different sizes.

Table 4. Size and impact event of NEOs.

D	H	Event	Impact Energy*	Frequency
25 m	25.76	Air burst	1 MT	200 yr
50 m	24.26	Local scale	10 MT	2,000 yr
140 m	22.02	Regional scale	300 MT	30,000 yr

* Megatons in TNT equivalent.

It is assumed to use visible telescope with a 2×2 deg^2 (1.2e-3 sr) Filed of View, FOV. Also it is assumed to survey the region corresponds to 30 deg of half angle (0.84 sr) from AEP in one day. Figure 12 shows the diagram of the daily survey from AEP. In this assumption, maximum exposure time, corresponding to the integration time, Δt, will be 125 sec. Note that the daily survey region described in Figure 12 is not optimal i.e., better survey strategy could be considered.

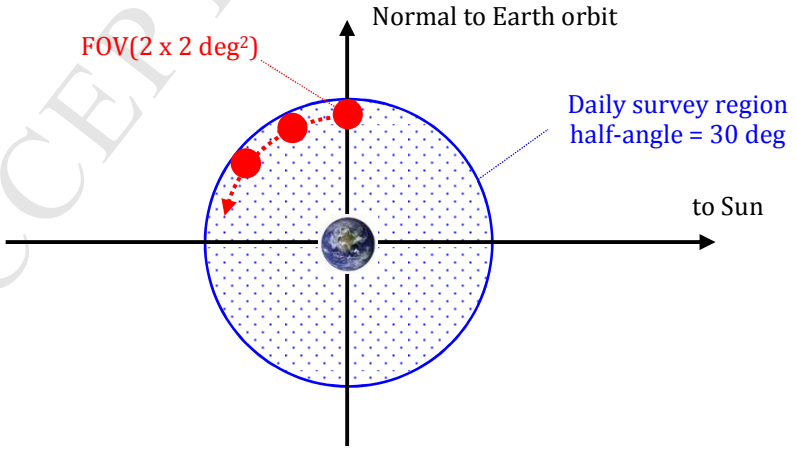

Fig. 12 Diagram of daily survey from AEP.

Three kinds of detector performance are assumed as summarized in Table 5. The aperture diameter, D_{ap} is calculated based on the detector performance of NEOSSat. In NEOSSat, D_{ap} = 15 cm, and the limiting magnitude is 20 at 100 sec exposure[19].

The definition of the apparent magnitude, the ratio of light intensity, ε is described as following;

$$\varepsilon^5 = 100 \tag{17}$$

which means 100 times larger light intensity is necessary to detect the object with "the limiting magnitude + 5" magnitude. In other word, 10 times larger mirror is needed. Then, the relationship between the two different mirrors can be described as following;

$$\frac{D_1}{D_2} = 10^{\frac{\Delta V}{5}} \tag{18}$$

where D_{ap1} and D_{ap2} are the aperture diameters.

Table 5. Detector performance

J_1	J (Δt = 125 sec)	D_{ap}
20	22.6	50 cm
22	24.6	125 cm
24	26.6	313 cm

VI Distribution in Telescopic View

This section shows VI's distribution in the telescopic view. Figure 13 shows the definition of the angles to describe the location of VI in the telescopic view.

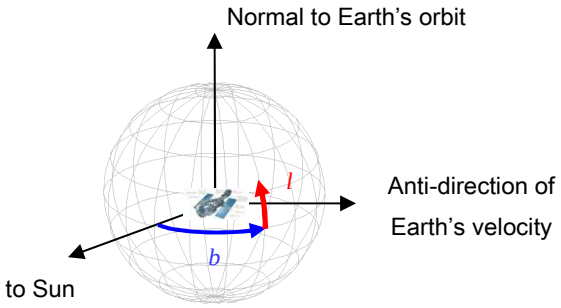

Fig. 13 Definition of Angles

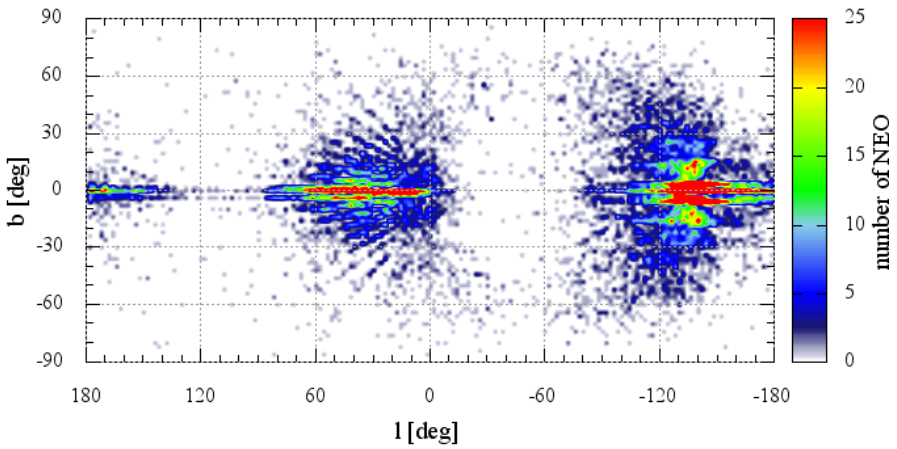

Fig 14. Distribution of VIs at 0.7 au

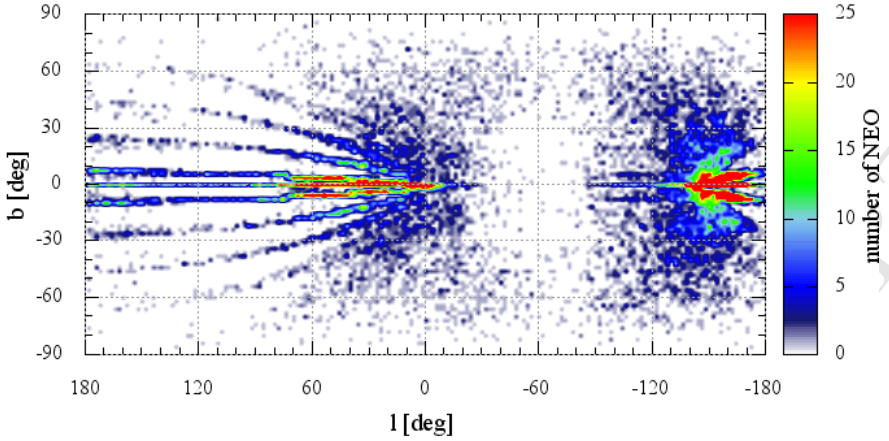

Fig 15. Distribution of VIs at 0.4 au

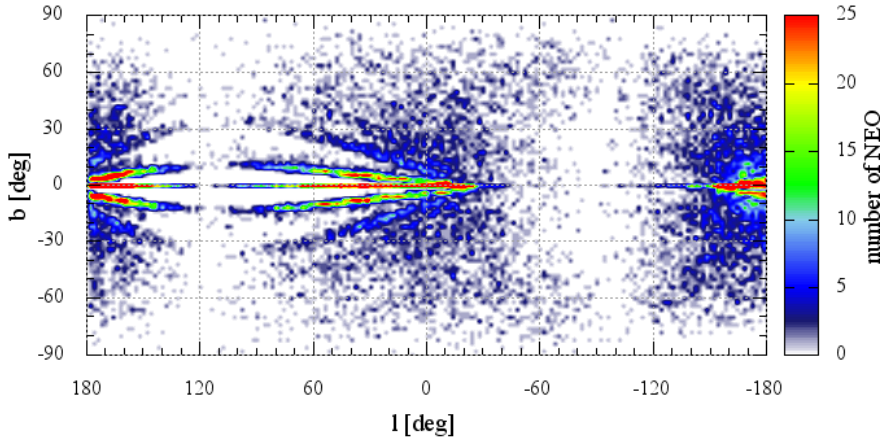

Fig 16. Distribution of VIs at 0.1 au

In this simulation, VI orbits are produced backwardly from Earth impact epoch until the distance between VI and Earth reaches designated value i.e., 0.7 au/0.4 au/ 0.1 au. To compare the results with SEL1 and AEP, Figure 14-16 show VI distributions of SEL1 case[36]. The center of the view is the direction from space telescope to Sun. When we see Figures 14-16, strange finger-like streaks can be found. The author thinks that this is because the inclination distribution of Bottke model is provided 5 deg step. As shown in Figures 14-16, VI distributions in the telescopic view “scatter” as VI approaching to Earth. This is because, the distance between SEL1 and Earth is only 0.01 au, therefore the angle of Line-of-Sight, LOS increases as VI approaching to Earth.

On the other hand, Figures 17-19 show VI distributions of AEP case. Note that the distances between VI and Earth of Figures 17-19 are fixed to 0.1 au, instead, AEP phase angle, α varies from 5 deg to 13 deg. The distances between telescopes on AEPs and Earth are from 0.09 to 0.22 au.

Detection Rate and Number of Detected VI

This section summarizes the summary of detection simulation in each detector performance shown in Table 5. Figures 20-22 show the rate of the detection percentage as function of the distance between VI and Earth in the case of J_1 = 20. α varies from 5 deg to 15 deg by 2 deg step.

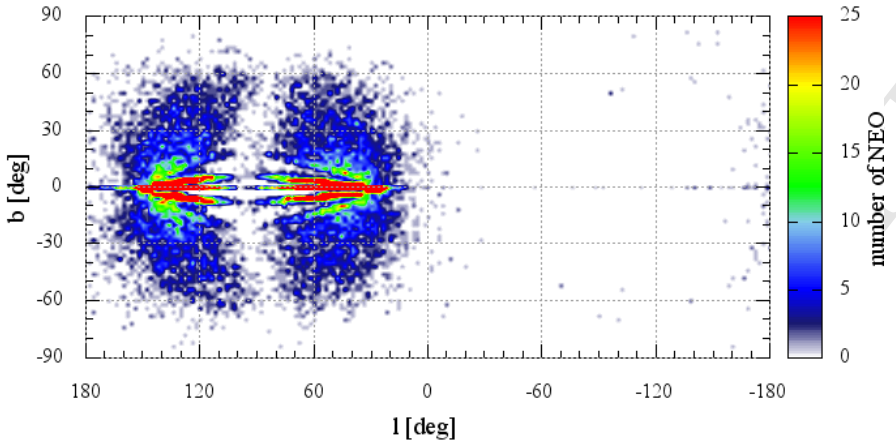

Fig 17. Distribution of VIs at 0.1 au: α = 5 deg

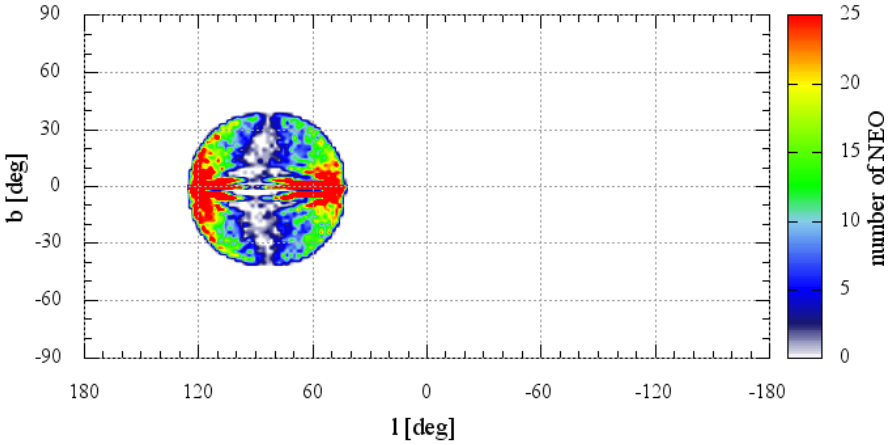

Fig 18. Distribution of VIs at 0.1 au: α = 9 deg

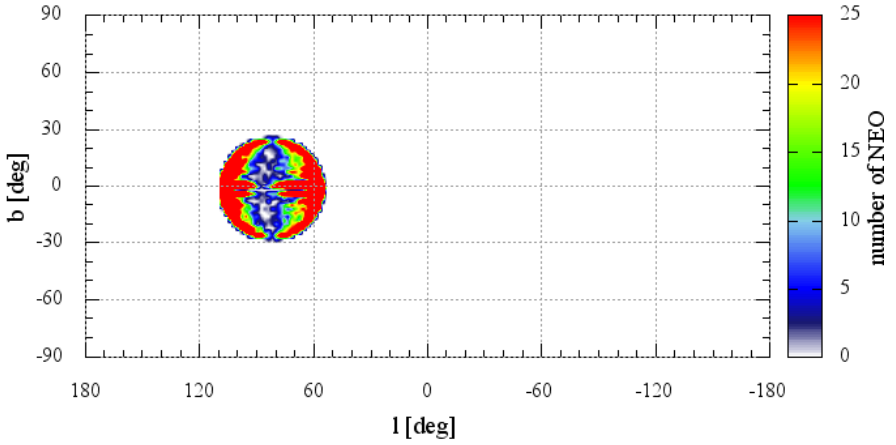

Fig 19. Distribution of VIs at 0.1 au: α = 13 deg

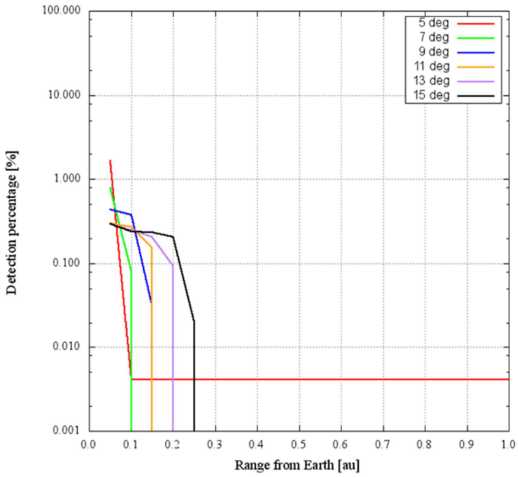

Fig. 20 Detection rate J_1 = 20 and D = 25 m

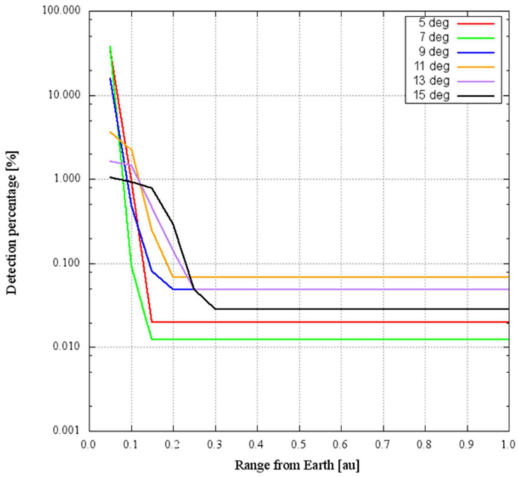

Fig. 21 Detection rate J_1 = 20 and D = 50 m

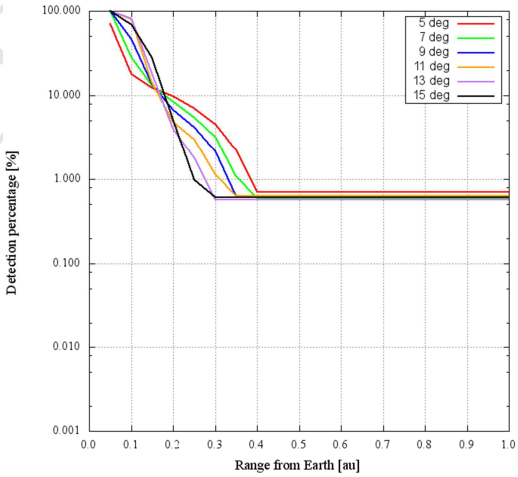

Fig. 22 Detection rate J_1 = 20 and D = 140 m

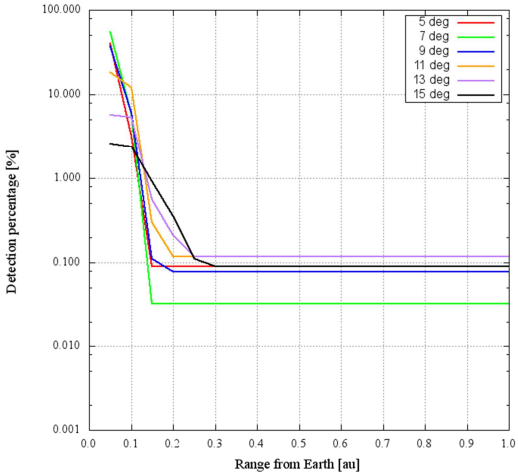

Fig. 23 Detection rate J_1 = 22 and D = 25 m

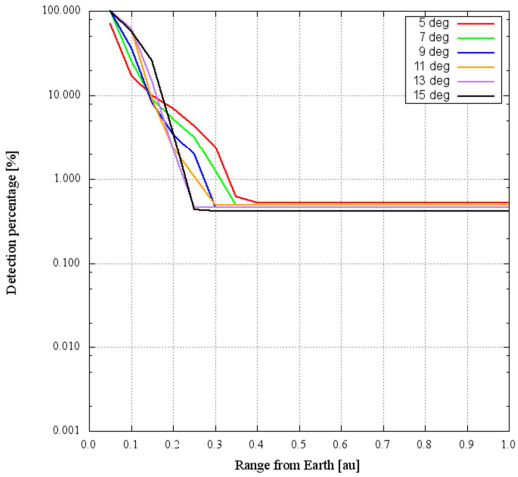

Fig. 24 Detection rate J_1 = 22 and D = 50 m

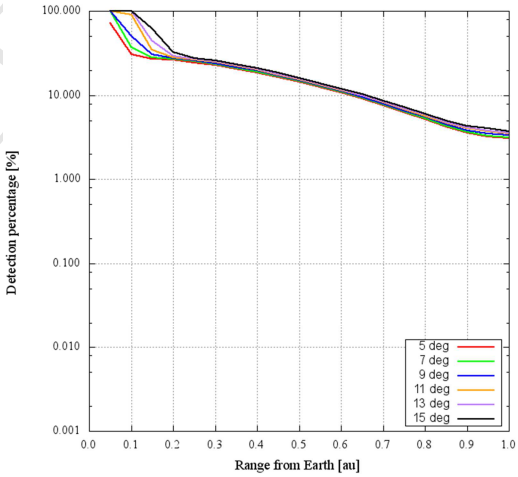

Fig. 25 Detection rate J_1 = 22 and D = 140 m

As shown, the detection rate rapidly increases when the distance between VI and Earth reaches roughly 0.2 – 0.3 au, this is because VIs concentrate into the survey region of AEP telescope.

Figures 23-25 show the detection rates in the case of J_1 = 22. In this case, the detection rate of 50 m size VIs reaches roughly 50% at 0.1 au, and almost 100% of 140 m VI can be detected at 0.1 au.

Figures 26-28 show the detection rates in the case of J_1 = 24. In this case, even 25 m VIs can be detected 100% at 0.1 au.

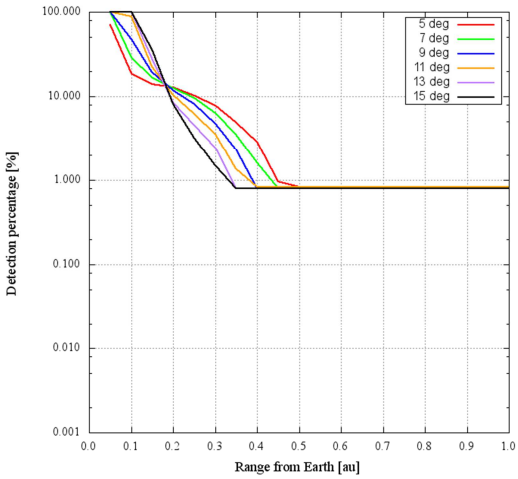

Fig. 24 Detection rate J_1 = 24 and D = 25 m

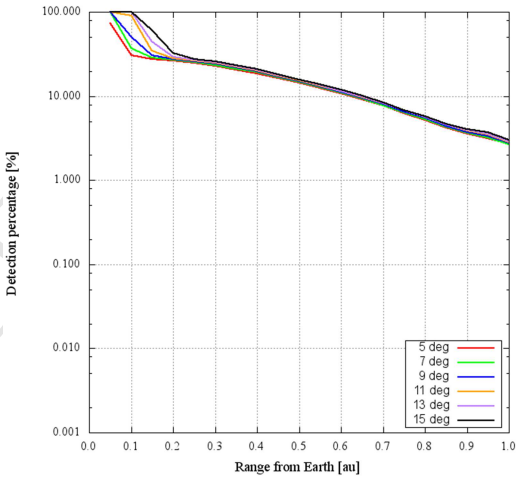

Fig. 24 Detection rate J_1 = 24 and D = 25 m

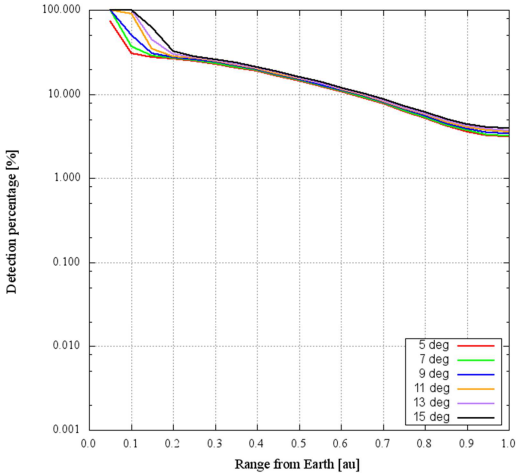

Fig. 24 Detection rate J_1 = 24 and D = 25 m

Lastly, Table 6 summarizes the detectability at 0.1 au. The percentage of Table 6 is the ratio of the detected VIs to the total number i.e., about 25,000.

Table 6. Summary of detectability

VI size		25 m	50 m	140 m
SEL1 (Case 2[36])*	J_1 = 20	0.1%	0.1%	5.1%
	J_1 = 22	0.1%	2.4%	42.3%
	J_1 = 24	9.0%	35.8%	52.4%
α = 5 deg	J_1 = 20	0.0%	1.0%	17.7%
	J_1 = 22	3.2%	17.2%	30.8%
	J_1 = 24	18.5%	30.9%	30.9%
α = 9 deg	J_1 = 20	0.4%	0.5%	46.0%
	J_1 = 22	6.1%	35.9%	50.6%
	J_1 = 24	47.8%	50.6%	50.7%
α = 13 deg	J_1 = 20	0.3%	1.5%	81.3%
	J_1 = 22	5.4%	61.6%	99.9%
	J_1 = 24	99.8%	99.8%	99.9%

* Case 2 surveys half sphere of the noon-side from SEL1[36]

Conclusion

This paper evaluated the performance of hazardous NEO detection mission using AEP. The results of SEL1 option conducted earlier were compared with those of AEP option. Consequently, the results of this study indicated that AEP has potential to detect all of Chelyabinsk-class impactors prior to the impact. However, it should be noted that low-thrust propulsion such as electric propulsion or solar sail is necessary to maintain the AEP location, which increases the mission cost.

Acknowledgement

The author would like to thank Mr. Martin Jocqueviel and Mr. Alessandro Takeshi Morita Gagliardi. They spent two months as Interns at JAXA and participated in the study. Their excellent results during the Internship has brought key factors to proceed the study.

References

[1] C. F. Chyba, P. J. Thomas, and K. J. Zahnle, “The 1908 Tunguska explosion: atmospheric disruption of a stony asteroid”, Nature, Vol. 361, 7 January, 1993.

[2] P. G. Brown, J. D. Assink, L. Astiz, R. Blaauw, M. B. Boslough, J. Borovicka, N. Brachet, D. Brown, M. Campbell-Brown, L. Ceranna, W. Cooke, C. de Groot-Hedlin, D. P. Drob, W. Edwards, L. G. Evers, M. Garces, J. Gill, M. Hedlin, A. Kingery, G. Laske, A. Le Pichon, P. Mialle, D. E. Moser, A. Saffer, E. Silber, P. Smets, R. E. Spalding, P. Spurny, E. Tagliaferri, D. Uren, R. J. Weryk, R. Whitaker, and Z. Krzeminski
, “A 500-kiloton airburst over Chelyabinsk and an enhanced hazard from small impactors”, 238, Nature, Vol. 503, 14 November, 2013.

[2] T. L. Edward, H. Reitsema, J. Troeltzsch, and S. Hubbard, “The B612 Foundation Sentinel Space Telescope”, Mary Ann Liebert, Inc., Vol. 1, No. 1, 2013.

[3] V. V. Emel’yanenko, O. P. Popova, N. N. Chugai, M. A. Shelyakov, Yu. V. Pakhomov, B. M. Shustov, V. V. Shuvalov, E. E. Biryukov, Yu. S. Rybnov, M. Ya. Marov, L. V. Rykhlova, S. A. Naroenkov, A. P. Kartashova, V. A. Kharlamov, and I. A. Trubetskaya, “Astronomical and Physical Aspects of the Chelyabinsk Event (February 15, 2013),” Solar System Research, Vol. 47, No. 4, pp. 240-254, 2013.

[4] J. I. Zuluaga, I. Ferrin, “A Preliminary Reconstruction of the Orbit of the Chelyabinsk Meteoroid,” Cornell University Library, 2013.

[5] W.F. Huebner, L. N. Johnson, D. C. Boice, P. Bradley, S. Chocron, A. Ghosh, P. T. Giguere, R. Goldstein, J. A. Guzik, J. J. Keady, J. Mukherjee, W. Patrick, C. Plesko, J. D. Walker, and K. Wohletz, “A Comprehensive Program for Countermeasures Agains Potentially Hazardous Objects (PHOs)”, Solar System Research, Vol. 43, No. 4, pp. 334-342, 2009.

[6] A. W. Harris, “NEA populations and impact frequency”, Asteroid Grand Challenge, Seminar Series, March 28, 2014.

[7] A. W. Harris, G. D’Abramo, “The near Earth asteroids”, Icarus, Vol. 257, September 2015, pp. 302-312, 2015.

[8] T. Spahr, “International Asteroid Warning Network: Recent Updates and MPC Summary,” Presentation to International Asteroid Warning Network Steering Committee, 2014.

[9] Association of Space Explorers Secure World Foundation CRECTEALC, “NEO IAWN Workshop Summary,” UN COPUOS STSC, 2010.

[10] L. Johnson, G. Drolshhagen, “Status of the International Asteroid Warning Network (IAWN), Space Mission Planning Advisory Group (SMPAG),” IAWN/SMPAG Report, 2015.

[11] National Research Council of the National Academies, Defending Planet Earth: Near-Earth Object Surveys and Hazard Mitigation Strategies Final Report, The National Academies Press, 2010.

[12] G. H. Stokes, J. B. Evans, S. M. Larson, “Near-Earth Asteroid Search Programs”, Asteroid III, pp. 45-54, 2002.

[13] L. Johnson, “International Asteroid Warning Network (IAWN) Status Report to STSC 2017”, Status Report to STSC, 2017.

[14] S. Okumura, N. Takahashi, S. Nakano, A. Asami, K. Nishiyama, S. Urakawa, T. Sakamoto, N. Hashimoto, M. Yoshikawa, “Spaceguard Activity in Japan: Past and Future in Bisei Spaceguard Center”, Asteroids, Comets, Meteors 2012, LPI Contribution No. 1667, id.6274, 2012.

[15] M. Yoshikawa, N. Takahashi, J. Watanabe, “Asia-Pacific Asteroid Observation Network”, 4th IAA Planetary Defense Conference, PDC 2015, IAA-PDC-15-01-05, 2015

[16] A. N. Heinze, J. L. Tonry, L. Denneau, H. Flewelling, B. Stalder, A. Rest, K. W. Smith, S. J. Smartt, and H. Weiland, “A First Catalog of Variable Stars Measured by the Asteroid Terrestrial-impact Last Alert System (ATLAS)”, Cornell University Library, Solar and Stellar Astrophysics, arXiv:1804.02132, 2018.

[17] A. K. Mainzer, P. Eisenhardt, E. L. Wright, F. C. Liu, W. Irace, I. Heinrichsen, R. Cutri, V. Duval, “Preliminary Design of The Wide-Field Infrared Survey Explorer(WISE)”, Cornell University Library, Astrophysics, arXiv:astro-ph/0508246, 2005.

[18] A. Mainzer, T. Grav, J. Bauer, J. Masiero, R. S. McMillan, R. M. Cutri, R. Walker, E. Wright, P. Eisenhardt, D. J. Tholen, T. Spahr, R. Jedicke, L. Denneau, E. DeBaun, D. Elsbury, T. Gautier, S. Gomillion, E. Hand, W. Mo, J. Watkins, A. Wikins, G. L. Bryngelson, A. Del Pino Molina, S. Desai, M. Gomez Camus, S. L. Hidalgo, I. Konstantopoulos, J. A. Larsen, C. Maleszewski, M. A. Malkan, J. C. Mauduit, B. L. Mullan, E. W. Olszewski, J. Pforr, A. Saro, J. V. Scotti, and L. H. Wasserman, “NEOWISE Observations of Near-Earth Objects: Preliminary Results”, The Astrophysical Journal, 743:156 (17pp), 2011 December 20, 2011.

[19] D. Laurin, A. Hildebrand, R. Cardinal, W. Harvey, S. Tafazoli, “NEOSSat – A Canadian Small Space Telescope for Near Earth Asteroid Detection”, Space Telescopes and Instrumentation 2008, doi: 10.1117/12.789736, 2008.

[20] CSA, “Evaluation of the Near Earth Object Surveillance Satellite (NEOSSat) Project”, Project # 13/14 02-02, 2014.

[21] C. Lewicki, P. Diamandis, E. Anderson, C. Voorhees, and F. Mycroft, “Planetary Resources – The Asteroid Mining Company”, Mary Ann Liebert, Inc. Vol. 1, No. 2, DOI: 10.1089/space.2013.0013, 2013.

[22] https://www.planetaryresources.com/2018/01/arkyd-6-is-in-orbit/, Planetary resources Inc. News, accessed in April 2018.

[23] H. Murakami, H. Baba, P. Barthel, D. L. Clements, M. Cohen, Y. Doi, K. Enya, E. Figueredo, N. Fujishiro,, H. Fujiwara, , M. Fujiwara, P. Garcia-Lario, T. Goto, S. Hasegawa, Y. Hibi, T. Hirao, N. Hiromoto, S. S. Hong, K. Imai, M. Ishigaki, M. Ishiguro, D. Ishihara, Y. Ita, W. S. Jeong, K. S. Jeong, H. Kaneda, H. Kataza, M. Kawada, T. Kawai, A. Kawamura, M. F. Kessler,D. Kester, T. Kii, D. C. Kim, W. Kim, H. Kobayashi,B. C. Koo, S. M. Kwon, H. M. Lee, R. Lorente, S. Makiuti, H. Matsuhara, T. Matsumoto, H. Matsuo, S. Matsuura, T. G. M. Ller, N. Murakami, H. Nagata, T. Nakagawa, T. Naoi, M. Narida, M. Noda, S. H. Oh, A. Ohnishi, Y. Ohyama, Y. Okada, H. Okuda, S. Oliver, T. Onaka, T. Ootsubo, S. Oyabu, S. Pak, Y. S. Park, C. P. Pearson, M. Rowan-Robinson, T. Saito, I. Sakon, A. Salama, S. Sato, R. S. Savage, S. Serjeant, H. Shibai, M. Shirahata, J. Sohn, T. Suzuki, T. Takagi, H. Takahashi, T. Tanabe, T. T. Takeuchi, S. Takita, M. Thomson, K. Uemizu, M. Ueno, F. Usui, E. Verdugo, T. Wada, L. Wang, T. Watabe, H. Watarai, G. J. White, I. Yamamura, C. Yamauchi, and A. Yasuda, “The Infrared Astronomical Mission AKARI”, Publ. Astron. Soc. Japan 59, S369–S376, 2007.

[24] V. Alí-Lagoa, T. G. Müller, F. Usui, and S. Hasegawa, “The AKARI IRC asteroid flux catalogue: updated diameters and albedos”, Astronomy & Astrophysics manuscript no. akari_NEATM, December 22, 2017.

[25] A. Mainzer, “NEOCam The Near-Earth Object Camera”, JPL, SBAG 2009 Nov. 18, 2009.

[26] E. T. Lu, H. Reitsema, J. Troeltzsch, and S. Hubbard, “The B612 Foundation Sentinel Space Telescope”, Mary Ann Liebert, Inc. Vol. 1, No. 1, DOI: 10.1089/space.2013.1500, 2013.

[27] M. Leipold, A. V. Richter, G. Hohn, A. W. Harris, E. Kuhrt, H. Michaelis, S. Mottola, “EARTHGUARD-I: A NEO Detection Space Mission”, Proceedings of Asteroids, Comets, Meteors (ACM 2002), 2002.

[28] Kayser-Threde GmbH, German Aerospace Center (DLR), “EARTHGUARD-I A Space-Based NEO Detection System”, Executive Summary, January, 2003.

[29] J. P. Gardner, J. C. Mather, M. Clampin, R. Doyon, M. A. Greenhouse, H. B. Hammel, J. B. Hutchings, P. Jakobsen, S. J. Lilly, K. S. Long, J. I. Jonathan, I. Lunine, M. J. Mccaughrean, M. Mountain, J. Nella, G. H. Rieke, M. J. Rieke, H. W. Rix, E. P. Smith, G. Sonneborn, M. Stiavelli, H. S. Stockman, R. A. Windhorst, and G. S. Wright, “The James Webb Space Telescope”, Space Science Reviews (2006) 123: 485–606, DOI: 10.1007/s11214-006-8315-7, Springer, 2006.

[30] M. A. Greenhous, “The James Webb Space Telescope: Mission Overview and Status”, AIAA SPACE 2012 Conference & Exposition, AIAA 2012-5100, 2012.

[31] A. S. Rivkin, F. Marchis, J. A. Stranberry, D. Takir, C. Thomas, and the JWST Asteroids Focus Group, “Asteroids and the James Webb Space Telescope”, Colnell University Library, Earth and Planetary Astrophysics, arXiv:1510.08414, 2015.

[32] M. Stramacchia, C. Colombo, F. Bernelli-Zazzera, “Distant Retrograde Orbits for space-based Near Earth Objects detection”, Advances in Space Research 58 (2016) 967-988, 2016.

[33] E. Perozzi, M. Ceccaroni, G. B. Valsecchi, and A. Rossi, “Distance retrograde orbits and the asteroid hazard”, The European Physical Journal Plus, 132: 367, 2017.

[34] A. Shugarov, B. Shustov, S. Naroenkov, M. Zvereva, “System of Observation of Day-Time Asteroids (SODA),” 5th IAA Planetary Defense Conference – PDC 2017, IAA-PDC-17-02-P02, 2017.

[35] B. Shustov, Yu.Makarov, S. Naroenkov, I.E.Molotov, M.Eselevich, M.Panasyuk, V. Shuvalov, M.Savel’ev, “Activities in Russia on NEO: Progress in Instrumentation, Study of Consequences and Coordination”, 5th IAA Planetary Defense Conference – PDC 2017, IAA-PDC-17-01-06, 2017.

[36] T. Ikenaga, A. T. M. Gagliardi, H. Ikeda, Y. Sugimoto, M. Utashima, N. Ishii and M. Yoshikawa, “Mission Design for NEO Detection and Impact Warning System,” Transaction of the Japan Society of Aeronautical and Space Sciences, Vol. 59, No. 4, pp. 243-250, 2016.

[37] W. F. Bottke Jr, A. Morbidelli, R. Jedicke, J. M. Petit, H. F. Levison, P. Michel, and T. S. Metcalfe, “Debiased Orbital and Absolute Magnitude Distribution of the Near-Earth Objects,” Icarus 156, 399-433, 2002.

[38] M. Granvik, A. Morbidelli, R. Jedicke, B. Bolin, W. F. Bottke, E. Beshore, D. Vokrouhlický, M. Delbò, and P. Michel, “Super-catastrophic disruption of asteroids at small perihelion distances”, doi:10.1038/nature16934, Nature volume 530, pages 303–306, 2016.

[39] ESA/ESTEC, “Final Report NEOPOP Near Earth Objects Population Observation Program”, SGNEOP_FR, revision 1.4, 2015.

[40] D. L. Mathias, L. F. Wheeler, J. L. Dotson, “A probabilistic asteroid impact risk model: assessment of sub-300 m impacts”, Icarus 289 (2017) 106–119, 2017.

[41] T. Yanagisawa, H. Kurosaki, “Detection of Faint GEO Objects using JAXA’s Fast Analysis Methods”, Trans. JSASS Aerospace Tech. Japan, Vol. 10, No. ists28, pp. Pr_29-Pr_35, 2012

[42] http://www.kenkai.jaxa.jp/pickup/neo-201803.html, JAXA/RDD news, accessed in April 2018 (in Japanese).

[43] M. Morimoto, H. Yamakawa, and K. Uesugi, “Periodic Orbits with Low-Thrust Propulsion in the Restricted Three-Body Problem”, Journal of Guidance, Control, and Dynamics, Vol. 29, No. 5, September–October 2006.

[44] R. Dymock, “The H and G Magnitude System for Asteroids”, The BAA Observer’s Workshops, J. Br. Astron. Assoc., 117 (2007), p.6, 2007.
[45] P. Veres, R. Jedicke, R. Wainscoat, M. Granvik, S. Chesley, S. Abe, L. Denneau and T. Grav, “Detection of Earth-Impacting Asteroids with the Next Generation All-Sky Surveys,” Icuras 203, 472-485, 2009.

[46] Y. Sugimoto, Hazardous Asteroids Mitigation: Campaign Planning and Credibility Analysis, Ph. D. dissertation, University of Glasgow, 2014

[47] M. Utashima, Simulation of NEO Detection by Space and Ground Telescope, NASDA-TMR-980003, 1999 (in Japanese).

- This is a concept study of a hazardous NEO detection and impact warning system.
- It is assumed to use space-based telescopes to detect virtual impactors before the impact.
- Sun-Earth L1 point and Artificial Equilibrium Point are used for space-telescope .
- SEL1 case shows the deficiency to detect NEOs in-coming from Sun-direction.
- On the other hand, AEP case shows almost 100% detectability of NEOs.